PHYSICAL REVIEW A **86**, 015401 (2012)

Conditions for extracting photoionization cross sections from laser-induced high-order-harmonic spectra

Guoli Wang,[1,2] Cheng Jin,[2] Anh-Thu Le,[2] and C. D. Lin[2]

[1]*Key Laboratory of Atomic and Molecular Physics and Functional Materials of Gansu Province, College of Physics and Electronic Engineering, Northwest Normal University, Lanzhou 730070, China*

[2]*J. R. Macdonald Laboratory, Physics Department, Kansas State University, Manhattan, Kansas 66506-2604, USA*

(Received 29 February 2012; published 10 July 2012)

We show that photoionization cross sections of atoms can be accurately extracted from the high-order-harmonic spectra generated by intense infrared lasers only if the degree of ionization in the gas medium is small, implying that for this purpose the high-order-harmonic generation spectra should be taken at low gas pressure and at low laser intensity experimentally.

DOI: 10.1103/PhysRevA.86.015401 PACS number(s): 32.80.Rm, 42.65.Ky

In a recent paper, Shiner *et al*. [1] used the so-called high-order-harmonic spectroscopy to probe collective multielectron dynamics in Xe. By comparing the measured high-order-harmonic generation (HHG) spectra of Kr and Xe atoms generated by intense 1.8-μm lasers and assuming that the photoionization cross section (PICS) of Kr is known, they deduced the differential PICS of Xe from the laser-generated HHG spectra. The deduced PICS reveals the well-known strong peak around 100 eV (photon energy), in good agreement with the $5p$ partial PICS that has been previously measured with synchrotron radiation light sources [2]. In the parlance of photoionization, this enhancement is caused by the so-called intershell coupling [3] with photoionization from the $4d$ shell of Xe, which is a specific form of the many-electron correlation effect [4]. To employ the procedure used by Shiner *et al*. [1], a number of assumptions have to be made. In this Brief Report, we examine the validity of these assumptions.

The conceptual connection between HHG and PI is built on the well-known three-step model [5,6] for HHG. In the third step, photorecombination is the inverse of photoionization, and the photorecombination cross section (PRCS) is trivially related to the PICS via the principle of detailed balance. Recently, the three-step model has been cast in a more rigorous form, in the quantitative rescattering (QRS) theory [7–9]. According to QRS and some relevant works [10], the HHG by an atom or molecule is related to the PRCS σ^r by

$$S(\omega) \propto w(\omega)\sigma^r(\omega), \tag{1}$$

where $S(\omega)$ is the HHG power spectrum and $w(\omega)$ is the so-called returning electron wave packet. In fact, Eq. (1) has been established at the level of complex amplitudes; thus each quantity in the equation has a magnitude and a phase [8,9]. Unlike PICS from conventional measurements, the phase of each harmonic can be determined experimentally [11], from which the phase of photorecombination transition dipole moment can be obtained. The validity of Eq. (1) has been established in our previous works [12]. Since the harmonic spectrum extends over a broadband, the electron wave packet also covers a broadband where the energies of the electrons and photons are related by $\hbar\omega = I_P + E$, where ω is the angular frequency of the photon, I_P is the ionization energy of the atom, and E is the "incident" electron energy. According to QRS, σ^r is directly related to the laser-free PICS and does not depend on the properties of the laser. On the other hand, the shape of $w(\omega)$ depends on the lasers only. Thus, at the "single-atom" level, according to QRS, for a fixed laser pulse, the ratio of the HHG spectra from two targets is the same as the ratio of their PRCS spectra. This forms the basis of the model used in Shiner *et al*. [1].

Experimentally, however, HHG spectra are generated coherently from all the atoms in the interaction region. The harmonics and the intense generating infrared laser field copropagate coherently in the medium before they reach the detector. Under favorable full phase-matching conditions the experimental HHG spectra grow quadratically with the number of gas atoms in the interaction region. If this assumption is correct, then the model used in Shiner *et al*. [1] is still valid. In practice, however, phase matching is very complicated. It depends on the focusing geometry, the induced dipole phase of each harmonic by the laser. It also depends on the dispersion and absorption of the atoms and the degree of ionization (plasma dispersion) of the medium by the laser (see [13] and references therein). (The HHG spectrum also depends on where and how the harmonics are measured, the position of the gas jet, and the pressure of the gas. Here we assume that they are the same for the two targets.) Extensive simulations have shown that full phase-matching conditions are never fulfilled, and they vary with harmonics. Despite these complications, however, simulations by Jin *et al*. [14] showed that Eq. (1) is still valid for HHG generated under the condition of low laser intensities and low gas pressure. In this case, Eq. (1) can be rewritten as

$$S_{\rm exp}(\omega) \propto W(\omega)\sigma^r(\omega), \tag{2}$$

where $S_{\rm exp}$ is the macroscopic HHG signal and $W(\omega)$ is interpreted as the "macroscopic wave packet" (MWP). At low pressure, dispersion and absorption are not important. At low intensity, there are few ionizations, so plasma dispersion is also not important. In this case, phase matching is governed by the laser focusing geometry and the induced atomic dipole, which depends mostly on the laser intensity only. In other words, the phase-matching conditions for the two targets are nearly identical, such that $W(\omega)$ for the two targets are essentially the same (see Fig. 5 of [14]), justifying the method used by Shiner *et al*. [1].

Shiner *et al*. [1] compared harmonic spectra using a laser intensity of 1.9×10^{14} W/cm^2 for Xe and 1.8×10^{14} W/cm^2 for Kr. One reason for this is to remove the shape of the returning electron wave packet. The other reason is that this normalization cancels out the instrument response of the XUV spectrometer. For Xe, the ionization potential is 12.13 eV, where the critical intensity is about 8.7×10^{13} W/cm^2 [15]. For Kr the ionization potential is 14 eV, and the critical intensity is 1.54×10^{14} W/cm^2. Here we define critical intensity to be the intensity where classical over-barrier ionization becomes possible. In both cases, the laser intensities used are quite high, with large degrees of ionization in the medium. The presence of a large amount of electrons in the gas medium causes plasma defocusing of the fundamental laser beam (see Fig. 2 in [16]). Since the degrees of ionization are quite different for the two targets, the resulting macroscopic wave packets $W(\omega)$ are quite different for Xe and Kr, thus making the procedure used in Shiner *et al*. [1] less accurate. Below we report our simulated results to quantify the error of the method.

In Fig. 1(a) we first show the wave packets $w(\omega)$ (the magnitude) for Xe and Kr from single-atom calculations at a peak laser intensity of 1.5×10^{14} W/cm^2. The wavelength is 1.8 μm, and pulse duration (FWHM) is 14 fs. The calculated wave packets have been averaged over the carrier-envelope phases (CEPs). Note that the two wave packets, after they have been normalized, are rather similar for the two different targets over the 20–160 eV range, thus validating Eq. (1) at the single-atom level.

To obtain HHG spectra that can be compared to experimental data, we solve the propagation of laser pulses and

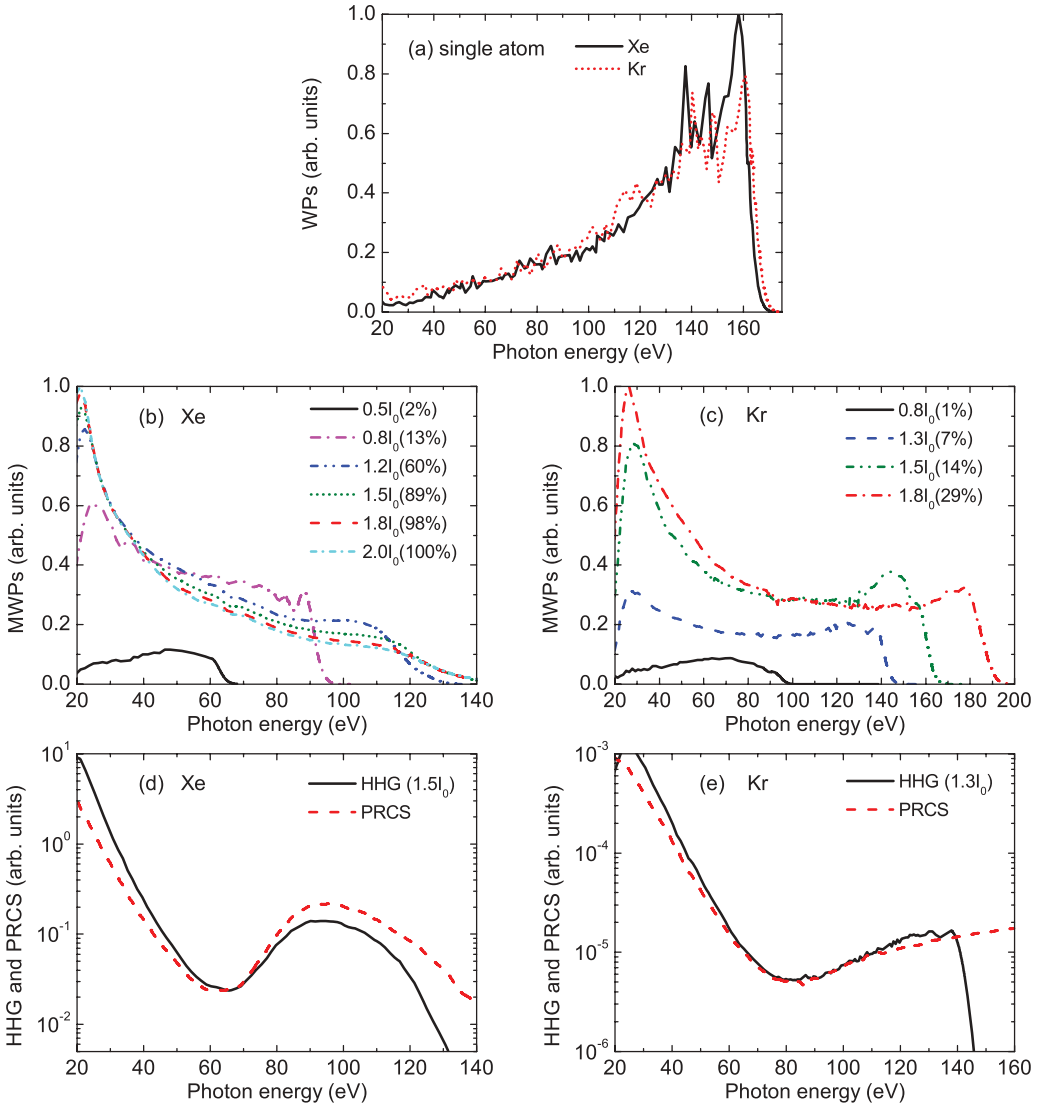

FIG. 1. (Color online) (a) The wave packets extracted from single-atom HHG spectra of Xe (solid line) and Kr [red (dotted) line] at a laser intensity of 1.5×10^{14} W/cm^2. (b) and (c) Dependence of macroscopic wave packets vs laser intensities given in units of $I_0 = 10^{14}$ W/cm^2. The numbers in parentheses are the ionization fractions at the end of the laser pulse for each intensity. (d) and (e) Comparison of the HHG spectrum (envelope) with PRCS [17,18] directly by normalizing at the spectral minimum. The peak intensities are 1.5 and 1.3×10^{14}W/cm^2 for Xe and Kr, respectively. The harmonics are generated in an $L_{\text{med}} = 0.5$ mm long gas jet and pressure of 6 Torr. Other laser parameters are given in the text.

harmonics in the medium [19–21] for conditions that include high pressure and high laser intensities. We assume that the spatial distribution of the laser intensity is Gaussian and laser beam waist is 100 μm. The gas jet has a density distribution [22] described by $\rho(z) = \rho_0 \exp(-5.55|z/L_{\rm med}|^3)$, where the gas-jet length is $2L_{\rm med} = 1$ mm and is placed at 1 mm after the laser focus. The harmonics are obtained after a slit with a width of 190 μm, placed 455 mm behind the focus, similar to the conditions used in [16,23]. From the calculated HHG spectra for each target, we obtain the MWPs.

In Figs. 1(b) and 1(c) we show the MWPs for each target at a few peak intensities. The degree of ionization for each intensity at the end of the laser pulse is given in parentheses. The ionization rates are calculated using the Ammosov-Delone-Krainov (ADK) theory [15,24]. First, we note that the ionization fraction in Kr is much smaller, thanks to its higher ionization potential. In the case of Kr, the MWP is very flat, and the cutoff is close to that given by $I_P + 3.2U_P$, where I_P is the ionization potential and U_P is the ponderomotive energy of the laser. For Xe, the degree of ionization is already quite large (60%) for an intensity of 1.2×10^{14} W/cm^2. At this intensity, the cutoff calculated from $I_P + 3.2U_P$ is ~129 eV, while the simulated spectrum shows that the cutoff is at 110 eV. At the other three higher intensities of 1.5, 1.8, and 2.0×10^{14} W/cm^2, none of the cutoff positions are sharp, and the position does not change with laser intensity. These behaviors are familiar for HHG generated using intensities well beyond the critical intensity (see Wang *et al.* [25] and references therein). Comparing the MWP in the same photon energy range for the two targets, we note that it is quite flat for Kr over a broad plateau energy region. For Xe, it drops by about a factor of 2 from 40 to 120 eV. Since the two wave packets are not similar, the procedure used in Shiner *et al.* [1] will introduce an error of a factor of about 2 in the extracted PRCS over the cited energy region.

An interesting observation from Fig. 1(c) is that the MWP remains fairly flat over a large plateau region for Kr where the ionization fractions are below 30%. If the MWP is flat, then according to Eq. (2), the HHG spectrum is directly proportional to the PRCS. In Fig. 1(e) we show that this is indeed the case to a high degree of accuracy. Here we normalize the two curves at the minimum. A similar comparison has been shown in Fig. 2 in Shiner *et al.* [1], where PICS and experimental HHG spectra were directly compared. If the same procedure is applied to Xe, as shown in Fig. 1(d), then a larger discrepancy occurs at the higher photon energy. Since the ionization fraction is already more than 60% at an intensity of 1.2×10^{14} W/cm^2, plasma defocusing reduces the field strength of the laser as it propagates, thus reducing the generation of higher harmonics. [The laser peak intensity (on axis) reduces to 1.07×10^{14} W/cm^2 at the exit of the gas jet for a CEP with a value of 0, which corresponds to a cutoff of ~115 eV according to $I_P + 3.2U_P$.] This reduction is reflected in the observed weak HHG signals as compared to PRCS if the two are normalized at the lower photon energy. The phase mismatch also plays an important role in the high-energy harmonics. The phase-mismatch values are calculated to be about 41, 103, and 124 mm^{-1} at photon energies of 40, 100, and 120 eV, respectively, for $z = 1$ mm and a laser intensity of 1.2×10^{14} W/cm^2. The big phase mismatch lowers the harmonic yield on the high-energy side of the spectrum. On the other hand, for Kr these values are 9, 23, and 28 mm^{-1}, respectively, under the same laser conditions.

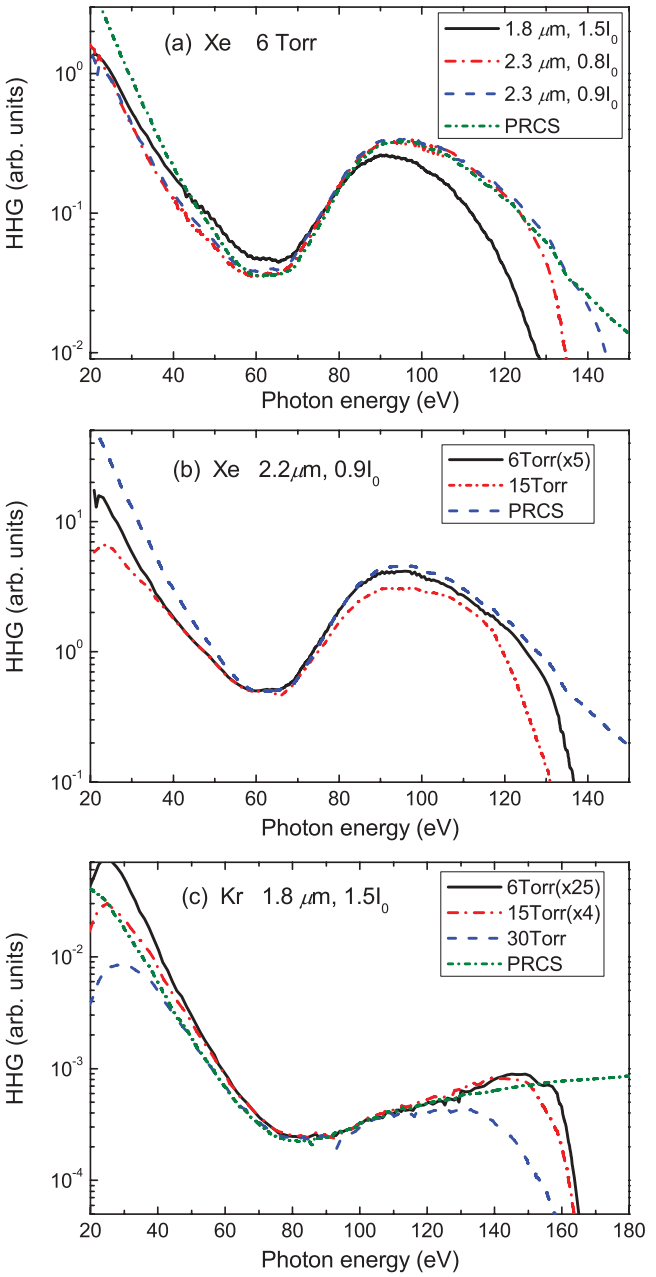

FIG. 2. (Color online) Effects of medium ionization on HHG spectra. (a) Comparison of PRCS with HHG spectra generated with different intensities and wavelengths for a fixed gas pressure. The PRCS and HHG that generated by 2.3 μm and $0.8I_0$ laser are normalized at their minima. The 1.8-μm curve has been scaled down by a factor of 16. (b) Effect of pressure on the HHG spectra in Xe. (c) Effect of pressure on the HHG spectra in Kr. Higher pressure can be used if the ionization potential is larger.

From the above analysis, it is clear that HHG spectra and PRCS would mimic each other if the medium is not severely ionized. For Xe, this can be done by using lasers with a longer wavelength but at lower peak intensity. Figure 2(a) compares the HHG generated using a 2.3-μm laser at intensities of 0.8

and 0.9×10^{14} W/cm^2. Also shown is the previous 1.8-μm result, where the yield has been scaled down by 16 times. (Here the total HHG signals are collected.) Figure 2(a) shows that the agreement of HHG and PRCS now extends over a larger energy region, up to about 130 eV, while the 1.8-μm data begin to deviate at about 85 eV. However, this is achieved at the expense of a reduction of a factor of 20 in the photon counts. In these simulations the gas pressure is fixed at 6 Torr. One possible way to increase the HHG yield is to increase the gas pressure. In Fig. 2(b) we show that the harmonic yield can increase by a factor of about 5 if the pressure is increased to 15 Torr. However, in doing so the density of the free electron quickly becomes too large, and the resulting HHG spectra again show the effect of plasma defocusing (or the effect of the saturation). The large absorption and dispersion in the range of 80–140 eV may also play an important role. Thus simply increasing the pressure would not do the trick. To maintain good phase matching, a new setup is needed, for example, using a waveguide [26]. When the ionization is smaller, as in the case of Kr [see Fig. 2(c)], increasing the pressure from 6 to 15 Torr enhances the harmonic yields by a factor of about 6, which is close to the quadratic dependence on the pressure, indicating that good phase matching is maintained in this pressure range. By doubling the pressure again, however, the plasma effect becomes significant, and the HHG and PRCS begin to deviate from each other quickly.

In summary, we address the experimental conditions under which photoionization cross sections can be extracted from laser-induced high-order-harmonic spectra. The method often used by experimentalists is to compare the HHG of an atomic target with that from a molecular target with nearly equal ionization potential. Based on our analysis, we have shown that the general condition for the validity of the method is that medium ionization (the absolute density of the free electron) should be small, typically for experiments carried out at low laser intensity and low gas pressure. We have further shown that the macroscopic wave packets in the plateau region using near-infrared lasers (say above 1.8 μm) are very flat. Thus if the medium ionization is small, then the PICS can be directly extracted from the HHG spectra without the need to compare it with an atomic target. When ionization in the medium is large, as in the experiment of Shiner *et al*. [1], the macroscopic wave packet is modified by the plasma effect, and then PICS can no longer be accurately retrieved from the HHG spectra in general. Thus to extract PICS from HHG spectra correctly, the simple condition is that medium ionization should be avoided as much as possible.

This work was supported in part by the Chemical Sciences, Geosciences and Biosciences Division, Office of Basic Energy Sciences, Office of Science, US Department of Energy. G.-L.W. was also supported by the National Natural Science Foundation of China under Grants No. 11064013 and No. 11044007 and the Specialized Research Fund for the Doctoral Program of Higher Education of China under Grant No. 20096203110001.

[1] A. D. Shiner, B. E. Schmidt, C. Trallero-Herrero, H. J. Wörner, S. Patchkovskii, P. B. Corkum, J.-C. Kieffer, F. Légaré, and D. M. Villeneuve, Nat. Phys. **7**, 464 (2011).
[2] U. Becker, D. Szostak, H. G. Kerkhoff, M. Kupsch, B. Langer, R. Wehlitz, A. Yagishita, and T. Hayaishi, Phys. Rev. A **39**, 3902 (1989).
[3] C. D. Lin, Phys. Rev. A **9**, 171 (1974).
[4] M. Ya. Amusia and J.-P. Connerade, Rep. Prog. Phys. **63**, 41 (2000).
[5] P. B. Corkum, Phys. Rev. Lett. **71**, 1994 (1993).
[6] M. Lewenstein, Ph. Balcou, M. Yu. Ivanov, A. L'Huillier, and P. B. Corkum, Phys. Rev. A **49**, 2117 (1994).
[7] T. Morishita, A. T. Le, Z. Chen, and C. D. Lin, Phys. Rev. Lett. **100**, 013903 (2008).
[8] A. T. Le, R. R. Lucchese, S. Tonzani, T. Morishita, and C. D. Lin, Phys. Rev. A **80**, 013401 (2009).
[9] C. D. Lin, A. T. Le, Z. Chen, T. Morishita, and R. R. Lucchese, J. Phys. B **43**, 122001 (2010).
[10] M. V. Frolov, N. L. Manakov, T. S. Sarantseva, and A. F. Starace, J. Phys. B **42**, 035601 (2009).
[11] P. M. Paul, E. S. Toma, P. Breger, G. Mullot, F. Augé, Ph. Balcou, H. G. Muller, and P. Agostini, Science **292**, 1689 (2001).
[12] A. T. Le, T. Morishita, and C. D. Lin, Phys. Rev. A **78**, 023814 (2008).
[13] C. Jin and C. D. Lin, Phys. Rev. A **85**, 033423 (2012).
[14] C. Jin, A. T. Le, and C. D. Lin, Phys. Rev. A **79**, 053413 (2009).
[15] X. M. Tong and C. D. Lin, J. Phys. B **38**, 2593 (2005).
[16] C. Jin, A. T. Le, C. A. Trallero-Herrero, and C. D. Lin, Phys. Rev. A **84**, 043411 (2011).
[17] M. Kutzner, V. Radojević, and H. P. Kelly, Phys. Rev. A **40**, 5052 (1989).
[18] K. N. Huang, W. R. Johnson, and K. T. Cheng, At. Nucl. Data Tables **26**, 33 (1981).
[19] P. Salières, A. L'Huillier, and M. Lewenstein, Phys. Rev. Lett. **74**, 3776 (1995).
[20] M. B. Gaarde, J. L. Tate, and K. J. Schafer, J. Phys. B **41**, 132001 (2008).
[21] C. Jin, A. T. Le, and C. D. Lin, Phys. Rev. A **83**, 023411 (2011).
[22] H. Dachraoui, T. Auguste, A. Helmstedt, P. Bartz, M. Michelswirth, N. Mueller, W. Pfeiffer, P. Salieres, and U. Heinzmann, J. Phys. B **42**, 175402 (2009).
[23] C. Trallero-Herrero, C. Jin, B. E. Schmidt, A. D. Shiner, J.-C. Kieffer, P. B. Corkum, D. M. Villeneuve, C. D. Lin, F. Légaré, and A. T. Le, J. Phys. B **45**, 011001 (2012).
[24] M. V. Ammosov, N. B. Delone, and V. P. Krainov, Zh. Eksp. Teor. Fiz. **91**, 2008 (1986) [Sov. Phys. JETP **64**, 1191 (1986)].
[25] G. Wang, C. Jin, A. T. Le, and C. D. Lin, Phys. Rev. A **84**, 053404 (2011).
[26] T. Popmintchev, M.-C. Chen, A. Bahabad, M. Gerrity, P. Sidorenko, O. Cohen, I. P. Christov, M. M. Murnane, and H. C. Kapteyn, Proc. Natl. Acad. Sci. USA **106**, 10516 (2009).